JPEDAV (2008) 29:300–304
DOI: 10.1007/s11669-008-9319-7
1547-7037 ©ASM International

Isothermal Sections in the (Fe, Ni)-Rich Part of the Fe-Ni-Al Phase Diagram

Igor Chumak, Klaus W. Richter, and Herbert Ipser

(Submitted November 14, 2007; in revised form March 4, 2008)

The ternary Fe-Ni-Al phase diagram below 50 at.% Al was investigated by a combination of powder x-ray diffraction (XRD) and electron probe microanalysis (EPMA). Ternary phase equilibria and accurate phase compositions of the respective equilibrium phases were determined within the partial isothermal sections at 900, 1000, 1100 and 1200 °C.

Keywords aluminum alloys, electron probe microanalysis (EPMA), experimental phase equilibria, x-ray analysis

1. Introduction

The large number of experimental investigations in the ternary Fe-Ni-Al system is caused by the wide range of applications of Fe-Ni-Al based alloys. The combination of the γ' with γ phase is the basis for the development of Ni-base superalloys.[1] The B2-type phase NiAl, on the other hand, is the starting point for the development of high-temperature alloys because of its high melting temperature and excellent oxidation resistance, but it is brittle at room temperature. The addition of disordered bcc α-(Fe-Al) and fcc γ-(Fe-Ni) phases improves the ductility of these alloys.[2]

The most recent critical assessment of the Fe-Ni-Al phase diagram was carried out by Eleno et al.[3] Isothermal sections of the Fe-Ni-Al phase diagram below 50 at.% Al were investigated long ago by Bradley[4,5] using x-ray powder diffraction and optical microscopy. Hao et al.[6] later reexamined the miscibility gap in Fe-Ni-Al by a diffusion couple technique. Jia et al.[7] examined the γ/γ' and γ'/B2 phase boundaries in Fe-Ni-Al, also by means of a diffusion couple method. Nevertheless, the phase relationships between α, γ and B2-phase are not established with sufficient accuracy.

The exact phase compositions in three-phase field [$\gamma' + \gamma +$ B2] at 1000 °C were recently determined from EPMA data by the present authors.[8] In this reference a vertical section Ni_3Fe-Ni_3Al is also given. The detailed investigation of phase equilibria in the Al-rich corner of the Fe-Ni-Al system using a combination of XRD, DTA, and EPMA was also published recently.[9]

Igor Chumak, Klaus W. Richter, and **Herbert Ipser,** Department of Inorganic Chemistry/Materials Chemistry, University of Vienna, Währingerstraße 42, A-1090 Vienna, Austria; **Igor Chumak,** Department of Inorganic Chemistry, Ivan Franko National University of Lviv, Kyryla and Mefodia str. 6, 79005 Lviv, Ukraine. Contact e-mail: chumak_i@yahoo.de

2. Experimental

Samples with a total mass of 1000 mg were prepared from aluminum rod (99.999%, Alfa, Karlsruhe, Germany), iron foil (99.99%, Advent Res., Halesworth, UK) and nickel foil (99.99%, Advent Res., Halesworth, UK). Calculated amounts of the elements were weighed to an accuracy of 0.05 mg and arc melted on a water-cooled copper plate under an argon atmosphere. Zirconium was used as a getter material within the arc chamber. The samples were re-melted one or two times and then weighed back in order to check for possible mass losses (which were generally found to be negligible). For equilibration the alloys were then annealed for 4 weeks at 900 °C, 2 weeks at 1000 °C, 4 days at 1100 °C and 12 h at 1200 °C. The samples were sealed into evacuated quartz glass ampoules (900-1100 °C) or into evacuated tantalum crucible (1200 °C). After quenching in water, the samples were investigated by means of x-ray diffraction (XRD) and electron microprobe analysis (EPMA).

Sample powders for x-ray diffraction were prepared with a diamond file with subsequent stress annealing for 5-15 min. Initial sample characterization was performed by x-ray powder diffraction, using the Guinier technique ($CuK\alpha_1$ radiation). The unit cell parameters were refined by means of the program TOPAS V2.1.[10]

The composition of the individual phases was determined by EPMA on a Cameca SX electron probe 100 (Cameca, Courbevoie, France) using wavelength dispersive spectroscopy (WDS) for quantitative analyses and employing pure aluminum, iron and nickel as standard materials. The measurements were carried out at 15 kV using a beam current of 20 nA. Conventional ZAF matrix correction was used to calculate the final composition from the measured x-ray intensities.

3. Results and Discussion

The phase equilibria in the Fe-Ni-Al ternary system below 50 at.% Al at 900-1200 °C were studied on 28 samples. The results of XRD and EPMA analysis are summarized in Table 1. Note that the composition of the

Table 1 Phase compositions and lattice parameters of identified phases

Nominal composition, at.%						Phase composition determined by EPMA, at.%			
Fe	Ni	Al	Annealing T, °C	Phase identified	Strukturbericht symbol	Fe	Ni	Al	a, Å
7	65	28	900	B2	B2	8.0(1)	58.6(1)	33.4(1)	2.8648(1)
				γ	A1	6.7(1)	67.9(1)	25.4(1)	3.5819(1)
7	76	17	900	γ′	$L1_2$	6.9(1)	74.1(1)	19.0(1)	3.5663(1)
				γ	A1	10.3(1)	77.8(1)	11.9(1)	...[a]
15	70	15	900	γ′	$L1_2$				3.5738(1)
20	60	20	900	B2	B2	15.0(2)	55.5(1)	29.5(1)	2.8676(1)
				γ′	$L1_2$	19.2(3)	61.3(1)	19.5(3)	3.5885(1)
				γ	A1	32.2(4)	55.3(4)	12.5(2)	...[a]
30	50	20	900	B2	B2	19.3(2)	51.3(1)	29.4(3)	2.8697(1)
				γ	A1	45.3(1)	44.9(1)	9.8(1)	3.5992(1)
40	40	20	900	B2	B2				2.8749(1)
				γ	A1				3.6024(1)
55	30	15	900	B2	B2	27.0(1)	41.8(3)	31.2(3)	2.8763(1)
				γ	A1	71.1(1)	21.9(1)	7.0(1)	3.5971(1)
74	15	11	900	B2	B2	39.6(7)	31.1(4)	29.3(3)	2.8749(1)
				γ	A1	80.7(3)	11.4(1)	7.9(2)	3.6269(4)
				α	A2	79.2(2)	10.0(2)	10.8(1)	...[b]
7	76	17	1000	γ′	$L1_2$	6.2	73.9	19.9	3.5684(1)
				γ	A1	9.1	76.9	14.0	...[a]
7	67	26	1000	B2	B2	7.6	60.9	31.5	2.8649(1)
				γ′	$L1_2$	6.7	68.7	24.6	3.5826(1)
15	62	23	1000	B2	B2	12.9	58.2	28.9	2.8658(1)
				γ′	$L1_2$	15.9	64.1	20.0	3.5864(1)
				γ	A1	23.5	61.3	15.2	...[a]
25	55	20	1000	B2	B2	17.2(1)	54.3(1)	28.5(1)	2.8676(1)
				γ	A1	34.8(3)	52.6(2)	12.6(1)	3.5937(1)
35	45	20	1000	B2	B2	23.5(2)	47.8(1)	28.7(3)	2.8730(1)
				γ	A1	51.8(4)	38.4(4)	9.8(1)	3.6070(1)
48	35	17	1000	B2	B2	28.5(2)	42.5(2)	29.0(1)	2.8765(1)
				γ	A1	63.7(3)	27.5(3)	8.8(1)	3.6030(1)
60	25	15	1000	B2	B2	36.4(5)	35.3(3)	28.3(2)	2.8794(1)
				γ	A1	72.6(1)	18.6(1)	8.8(1)	3.6036(1)
71	16	13	1000	B2	B2	63.7(2)	18.3(3)	18.0(3)	2.8736(1)
				γ	A1	77.1(2)	13.2(2)	9.7(1)	3.6210(6)
				α	A2	72.6(1)	13.5(1)	13.9(1)	...[b]
9	66	25	1100	B2	B2	9.5(1)	61.0(4)	29.5(4)	2.8634(1)
				γ′	$L1_2$	9.5(1)	67.7(2)	22.8(1)	3.5847(1)
10	72	18	1100	γ′	$L1_2$	9.0(1)	70.4(1)	20.6(1)	3.5830(1)
				γ	A1	13.4(1)	70.8(3)	15.8(3)	...[a]
15	64	21	1100	B2	B2	11.6(1)	59.7(2)	28.7(1)	2.8709(1)
				γ′	$L1_2$	13.5(1)	65.5(2)	21.0(2)	3.5944(1)
				γ	A1	19.5(2)	63.8(2)	16.7(2)	...[a]
42	41	17	1100	B2	B2	26.8(2)	45.3(1)	27.9(1)	2.8753(1)
				γ	A1	53.5(1)	35.8(1)	10.7(1)	3.6054(1)
67	20	13	1100	B2	B2	49.7(2)	26.9(1)	23.4(1)	2.8877(3)
				γ	A1	72.0(1)	11.3(1)	10.7(1)	3.6201(3)
68	17	15	1100	α	A2	68.4(2)	16.2(1)	15.4(1)	2.8853(1)
				γ	A1	74.3(1)	14.9(1)	10.8(1)	3.6305(6)
5	69	26	1200	B2	B2	5.3(1)	64.8(1)	29.9(1)	2.8607(1)
				γ′	$L1_2$	5.2(1)	70.7(1)	24.1(1)	3.5790(1)

Table 1 Continued

Nominal composition, at.%						Phase composition determined by EPMA, at.%			
Fe	Ni	Al	Annealing T, °C	Phase identified	Strukturbericht symbol	Fe	Ni	Al	a, Å
5	76	19	1200	γ′	$L1_2$	3.9(4)	73.0(4)	23.1(3)	3.5673(2)
				γ	A1	...	...	...	...[a]
11.5	67.5	21	1200	B2	B2	9.1(2)	60.9(4)	30.0(4)	2.8603(4)
				γ′	$L1_2$	8.7(2)	68.7(1)	22.6(5)	3.5794(1)
				γ	A1	13.2(1)	68.5(1)	18.3(1)	...[a]
13	66	21	1200	B2	B2	10.2(4)	60.0(4)	29.8(3)	Not determined
				γ	A1	15.2(2)	67.0(4)	17.8(2)	
41	41	18	1200	B2	B2	29.6(1)	43.5(1)	26.9(1)	2.8729(1)
				γ	A1	51.0(2)	36.5(2)	12.5(1)	3.6025(1)
64	22	14	1200	α	A2	57.0(1)	23.7(1)	19.3(1)	2.8743(1)
				γ	A1	67.2(2)	20.2(1)	12.6(1)	3.6025(1)

[a]Overlap with γ′
[b]Overlap with B2

γ-phase in two-phase sample $Fe_5Ni_{76}Al_{19}$, annealed at 1200 °C, could not be measured properly by EPMA due to the very fine microstructure of this sample. The phase compositions determined by EPMA were combined with diffusion couple literature data from Hao et al.[6] and Jia et al.[7] to yield the partial isothermal sections at 900-1200 °C (Fig. 1). Figure 2 shows, as examples, BSE images of two three-phase samples [γ′ + γ + B2], [α + B2 + γ] and one two-phase sample [B2 + γ] annealed at 900 °C.

The boundary composition of the γ′-Ni_3(Al, Fe) phase, determined in the three-phase field [γ′ + γ + B2], varies almost linearly with temperature (cf. Fig. 3). Its equilibrium composition (0.5 at.% Fe, 75 at.% Ni, 24.5 at.% Al) involved in the transition reaction U: L + γ′ = γ + B2 at 1366 ± 1 °C reported by Chumak et al.[8] fits well with this linear trend (Fig. 3). The three-phase field [α + B2 + γ], which is connected with the miscibility gap between disordered α and ordered B2-type phases, was detected

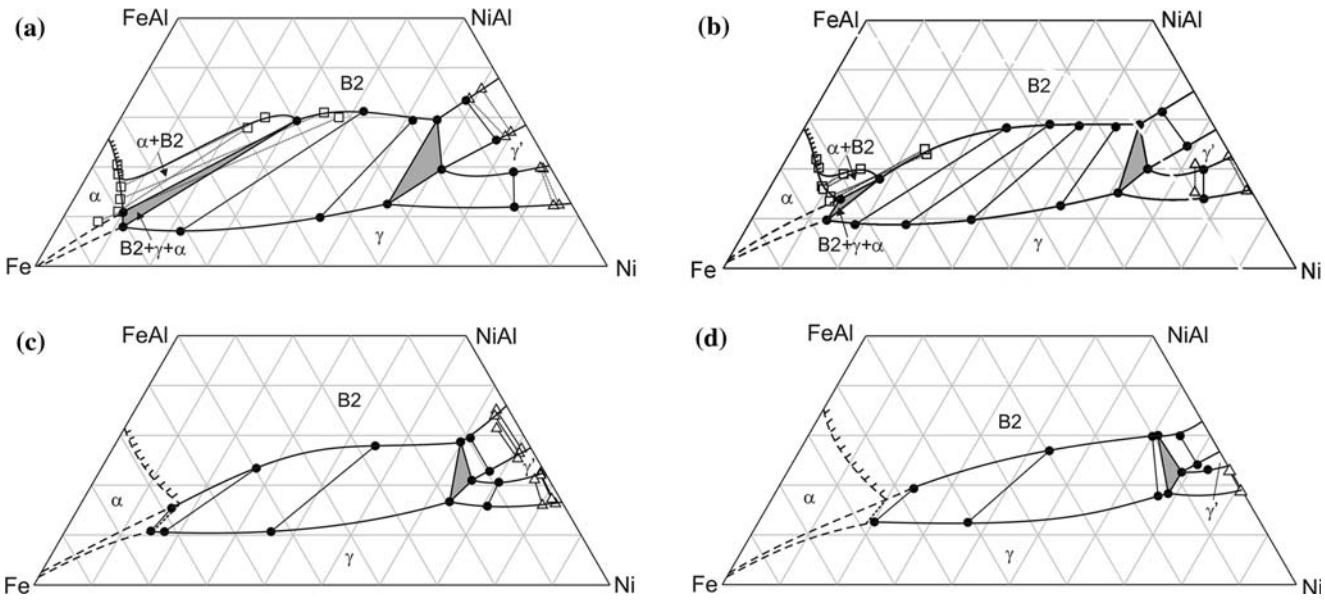

Fig. 1 Partial isothermal sections of Fe-Ni-Al with experimental tie-lines and triangles: (a) at 900 °C, (b) at 1000 °C, (c) at 1100 °C, (d) at 1200 °C. Black circles: phase compositions measured by EPMA; white squares: phase compositions in diffusion couples from Hao et al.[6]; white triangles: phase compositions in diffusion couples from Jia et al.[7]; hatched-full lines: second-order phase boundaries investigated by Hao et al.[6]; hatched-dashed lines: second-order phase boundaries extrapolated from the limiting binary Fe-Al

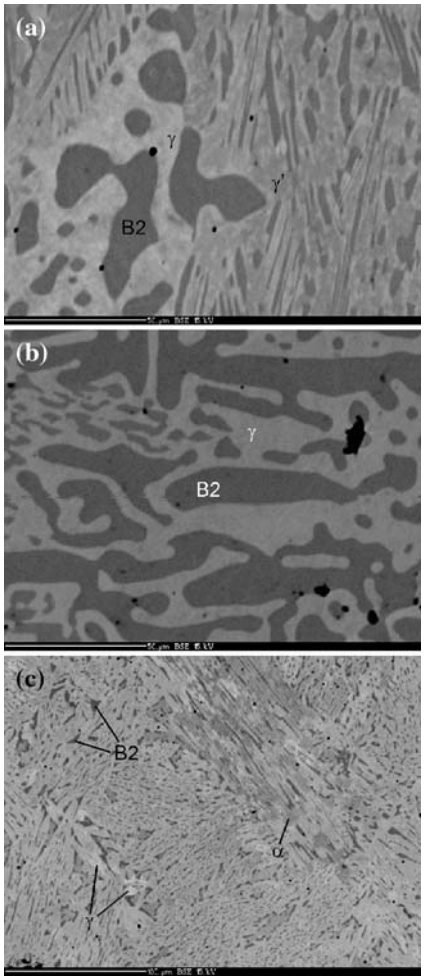

Fig. 2 BSE images of samples annealed at 900 °C. Sample compositions: (a) $Fe_{20}Ni_{60}Al_{20}$, (b) $Fe_{30}Ni_{50}Al_{20}$, (c) $Fe_{74}Ni_{15}Al_{11}$

only at 900 and 1000 °C. This result confirms the assumption of Eleno et al.[3] that the miscibility gap closes between 1050 and 1150 °C. Therefore, the lines symbolizing the second-order transition α → B2 at 1100 and 1200 °C are extrapolated from the limiting binary Fe-Al system (Fig. 1c, d). It should be pointed, that the composition of the α-phase in the three-phase field [α + B2 + γ] measured in this work (Fig. 1a, b), deviates significantly from the values given in the review of Eleno et al.[3]

In order to compare the results for the four isothermal sections reported here with our DTA investigation of the section Ni_3Al-Ni_3Fe reported previously,[8] the phase boundaries of the γ- and γ′-phases at 75 at.% Ni were evaluated graphically in all four isothermal sections. The resulting phase boundaries are shown in Fig. 4 which also includes our experimental DTA data[8] and DSC data given by Himuro et al.[11] As can be seen, the phase boundaries agree well at high temperatures (1200 °C), but they deviate considerably at lower temperatures. This fact may be interpreted as follows: the γ′ to [γ + γ′] transition and the [γ + γ′] to γ transition are solid-state phase reactions that

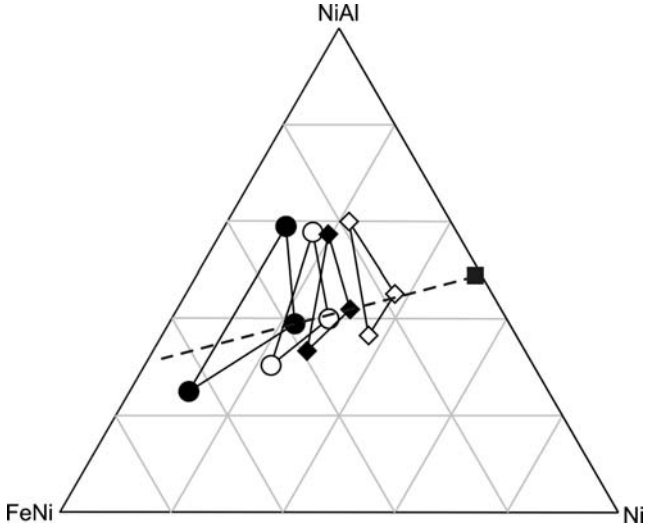

Fig. 3 The location of [γ′ + γ + B2] three-phase field at different temperatures: black circles—at 900 °C, white circles—at 1000 °C, black rhombs—at 1100 °C, white rhombs—at 1200 °C. The equilibrium composition of the γ′ phase involved in the transition reaction U: L + γ′ = γ + B2 at 1366 ± 1 °C[8] is marked with black square

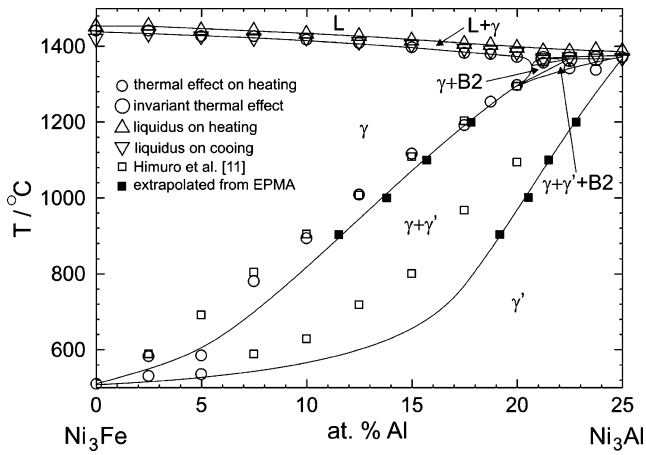

Fig. 4 Comparison of DTA[8] and DSC data[11] within the section Ni_3Fe-Ni_3Al with phase boundaries evaluated from the isothermal sections given in this work

involve diffusion processes in order to establish equilibrium. It may be assumed that these transitions are rather slow at low temperatures. Thus, the determination of these effects with dynamic methods like DTA and DSC, may result in a shift of the observed effect relative to the equilibrium value. As the effects were evaluated from the heating curves, we expect a shift towards higher temperatures. In fact, the data given in Fig. 4 support this hypothesis. As the data evaluated from the isothermal sections (black squares) were obtained from EPMA analysis of well-annealed samples, we conclude that these data are more reliable for the determination of the γ′ to [γ + γ′] transition and the [γ + γ′] to γ transition temperatures within the section Ni_3Al-Ni_3Fe.

Acknowledgments

Financial support from the Austrian Science Foundation (FWF), under the ''Lise-Meitner-Stipendium'', Project Number M906-B10, and financial support from COST 535 is gratefully acknowledged.

References

1. G. Sauthoff, Multiphase Intermetallic Alloys for Structural Applications, *Intermetallics*, 2000, **8**, p 1101-1109
2. D. Letzig, J. Klöwer, and G. Sauthoff, Screening of NiAl-base Ni-Fe-Al Alloys for Structural High Temperature Applications and Development of a New Ni-30Fe-10Al-Cr Alloy, *Z. Metallkd.*, 1999, **90**, p 712-721
3. L. Eleno, K. Frisk, and A. Schneider, Assessment of the Fe-Ni-Al System, *Intermetallics*, 2006, **14**, p 1276-1290
4. A.J. Bradley, Microscopical Studies on the Iron-Nickel-Aluminium System. Part I—$\alpha + \beta$ Alloys and Isothermal Sections of the Phase Equilibrium Diagram, *J. Iron Steel Inst.*, 1949, **163**, p 19-30
5. A.J. Bradley, Microscopical Studies on the Iron-Nickel-Aluminium System. Part II—the Breakdown of the Body-centered Cubic Lattice, *J. Iron Steel Inst.*, 1951, **168**, p 233-244
6. S.M. Hao, T. Takayama, K. Ishida, and T. Nishizawa, Miscibility Gap in Fe-Ni-Al and Fe-Ni-Al-Co Systems, *Metall. Trans. A.*, 1984, **15**, p 1819-1828
7. C.C. Jia, K. Ishida, and T. Nishizawa, Partition of Alloying Elements Between γ (A1), γ' ($L1_2$) and β (B2) Phases in Ni-Al Base Systems, *Metall. Mater. Trans. A.*, 1994, **25**, p 473-485
8. I. Chumak, K.W. Richter, S.G. Fries, and H. Ipser, Experimental Phase Diagram Investigations in the Ni-Rich Part of Al-Fe-Ni and Comparison with Calculated Phase Equilibria, *J. Phase Equilib. Diffus.*, 2007, **28**, p 417-421
9. I. Chumak, K.W. Richter, and H. Ipser, The Fe-Ni-Al Phase Diagram in the Al-rich (>50 at.% Al) Corner, *Intermetallics*, 2007, **15**, p 1416-1424
10. TOPAS V2.1, *General Profile and Structure Analysis Software for Powder Diffraction Data*, Bruker AXS, Karlsruhe, Germany, 2005
11. Y. Himuro, Y. Tanaka, N. Kamiya, I. Ohnuma, R. Kainuma, and K. Ishida, Stability of Ordered $L1_2$ Phase in Ni_3Fe-Ni_3X (X:Si and Al) Pseudobinary Alloys, *Intermetallics*, 2004, **12**, p 635-643